Healthcare Analytics 4 (2023) 100216

Contents lists available at ScienceDirect

Healthcare Analytics

journal homepage: www.elsevier.com/locate/health

A comprehensive review of deep neural networks for medical image processing: Recent developments and future opportunities

Pawan Kumar Mall [a,*], Pradeep Kumar Singh [b], Swapnita Srivastav [c], Vipul Narayan [c], Marcin Paprzycki [d], Tatiana Jaworska [d], Maria Ganzha [d]

[a] Lovely Professional University, Jalandhar - Delhi G.T. Road, Phagwara, Punjab 144411, India
[b] Department of Computer Science and Engineering, Madan Mohan Malaviya University of Technology, Gorakhpur, U.P, 273008, India
[c] Galgotias University, Greater Noida, India
[d] Systems Research Institute, Polish Academy of Sciences, Poland

ARTICLE INFO

Keywords:
Artificial intelligence
Deep neural networks
Predictive analytics
Machine learning
Medical imaging diagnostic analytics

ABSTRACT

Artificial Intelligence (AI) solutions have been widely used in healthcare, and recent developments in deep neural networks have contributed to significant advances in medical image processing. Much ongoing research is aimed at helping medical practitioners by providing automated systems to analyze images and diagnose acute diseases, such as brain tumors, bone cancer, breast cancer, bone fracture, and many others. This comprehensive review delivers an overview of recent advances in medical imaging using deep neural networks. In addition to the comprehensive literature review, a summary of openly available data sources and future research directions are outlined.

1. Introduction

Recent years can be characterized by rapid developments in the area of, broadly understood, artificial intelligence (AI). One of the subareas of AI that has reached real-world applicability is machine learning (ML). Here, some of the key developments involve neural networks (NN). It can be said that the development of artificial neural networks proceeds in a sinusoidal fashion. After an early interest in the late 1950s and early 1960s, a period of relative dormancy lasted till 1986, when James McClelland and David Rumelhart published their famous book [1]. This revived interest in neural network research. However, by the end of the 20th century, the interest in a neural networks has diminished again. One of the reasons for the stagnation was a lack of computer hardware capable of handling the amount of data needed to make obtainable neural network models actually applicable [2]. It is only in the last ten years that renewed interest in NNs resulted in the development of successful applications capable of addressing actual, real-life problems. Some of the neural network architectures that attracted a lot of interest in deep neural networks (DNNs). They have been implemented in many areas, such as medical image classification, electromyography recognition, disease recognition and segmentation, and many others. However, in this work, we are interested in providing an overview of the use of DNNs in medical imaging.

Deep neural networks (DNNs) have significantly improved diagnosis, treatment planning, and patient care by revolutionizing several facets of medical image processing. Their capacity to extract significant characteristics and patterns from medical image using large-scale datasets has demonstrated to be very successful, resulting in more precise and effective analysis [3]. DNNs are especially effective at tasks like image classification and segmentation, which are essential in medical imaging. Deep networks may learn to recognize and categorize different anatomical features, lesions, or anomalies in medical image by training on massive annotated datasets. Additionally, they can precisely divide up organs or other areas of interest, allowing for exact measurements and quantitative analysis. DNNs have been heavily included into computer-aided diagnostic (CAD) systems [4]. These networks may identify minor patterns or irregularities in medical images that may be difficult for human observers to notice by learning from enormous volumes of labeled data. DNN-based CAD solutions benefit radiologists and doctors by supplying more details and enhancing diagnostic precision. Deep learning algorithms have been effectively used for image restoration and enhancement jobs in the field of medicine [5]. For instance, DNNs may recreate high-quality image from imperfect or noisy data in computed tomography (CT) and magnetic resonance imaging (MRI), lowering artifacts and enhancing image quality. These developments result in quicker scans, lower radiation doses, and better

* Corresponding author.
E-mail addresses: Pawankumar.mall@gmail.com (P.K. Mall), topksingh@gmail.com (P.K. Singh), swapnitasrivastava@gmail.com (S. Srivastav), vipulupsainian2470@gmail.com (V. Narayan), paprzyck@ibspan.waw.pl (M. Paprzycki), tatiana.Jaworska@ibspan.waw.pl (T. Jaworska), m.ganzha@mini.pw.edu.pl (M. Ganzha).

https://doi.org/10.1016/j.health.2023.100216
Received 29 April 2023; Received in revised form 16 June 2023; Accepted 21 June 2023

anatomical structure visualization. Deep neural networks have been employed for accurate and robust image registration, which involves aligning multiple medical images acquired from different modalities or time points [6]. By learning spatial transformations, DNNs can automatically align images and facilitate comparisons, such as tracking disease progression or planning interventions. Disease Detection and Prediction: DNNs have shown promise in automated disease detection and prediction using medical images. By learning from large-scale datasets, these networks can identify specific imaging biomarkers associated with diseases. For example, in cancer imaging, DNNs can identify tumor characteristics, predict tumor malignancy, or assess treatment response based on radiological images. Deep neural networks can generate synthetic medical images, aiding in data augmentation, training set expansion, and creating realistic simulations for training and testing purposes. This synthesis of images is particularly useful in situations with limited annotated data or rare conditions, where DNNs can generate diverse examples to enhance the performance of models. Personalized Medicine and deep learning models can analyze medical images in conjunction with other clinical data, such as genomics or electronic health records, to enable personalized medicine. By integrating patient-specific information, DNNs can assist in treatment planning, prognostication, and selection of optimal therapies based on image-derived features and patterns.

The main structure of this article is: Section 2 an overview of deep neural network. Section 3 gives details about Medical image datasets organized according to organs. Section 4 gives details Medical image datasets organized according to organs. Section 5 states the researchChallenges and Future Directions Section 6 states the research conclusion of this article.

2. Deep neural networks

In general, a deep neural network (DNN) is a subset of Machine Learning (ML) that uses large multilayer neural networks. The key ideas behind these networks materialize in the form of algorithms, inspired by the way that the human brain deals with large amounts of data (for training). DNN algorithms perform a task over and over again, eventually improving the results as a result of the deep layers that allow progressive learning to occur. DNN is an architecture with a large number of, usually wide, layers between the input and output layers. For instance, currently, DNNs can have beyond 1200 layers and more than 16 million neurons [7]. Moreover, while these layers are not homogeneous, they all consist of neurons whose function is modeled after actual neurons by an activation function (non-linear or linear) [8], such as hyperbolic tangent, sigmoid, etc. There are some basic layers according to the roles that they have in different architectures. The layer where the extraction of features takes place is a convolutional layer, the name of which comes from the convolution operations performed using different filters. There exists a large number of specific DNN architectures [9]. Let us summarize the main ones. The interested reader should consult the cited works for more detail, including a representation of each architecture.

Deep neural networks (DNNs) have indeed been widely used to improve the efficiency of pattern recognition tasks in various organs or anatomical regions within medical imaging. These DNN models have shown promising results in areas such as kidney, liver, brain, bone, breast, chest, eyes, and more. They have the potential to provide accurate and automated analysis of medical images, aiding in diagnosis, treatment planning, and monitoring of diseases [10].

The hierarchical representation of medical images and analyses using deep neural networks typically involves several stages. Fig. 1 (not provided) likely illustrates this hierarchy, which I can describe in general terms.

At the bottom row of the hierarchy, different types of modalities are used for training the DNN models. These modalities can include imaging techniques such as magnetic resonance imaging (MRI), computed tomography (CT), positron emission tomography (PET), ultrasound, and X-ray, among others. Each modality provides unique information about the anatomical structures or physiological processes being studied.

The DNN models are trained using large datasets of labeled medical images corresponding to the specific modality or modalities being used. These datasets are crucial for the DNNs to learn patterns and features relevant to the desired tasks. The training process involves optimizing the network's parameters through techniques like backpropagation and gradient descent, allowing the model to learn how to accurately classify, segment, or detect specific features in the medical images [11].

Once the DNN models are trained, they can be used for various analyses on unseen medical images. This can include tasks such as image classification, where the DNN identifies the presence or absence of certain anatomical or pathological features. It can also involve image segmentation, where the DNN identifies and delineates specific structures or regions within the image. Additionally, DNNs can be employed for object detection, where they locate and localize multiple instances of specific objects or abnormalities within the image.

The detailed study [12] on GAN-based medical image enhancement. The problem of small training sample sizes for medical image diagnostic and treatment models is well solved by this strategy. The amount of training samples for models of medical image-based diagnosis and therapy is growing as deep learning progresses. Due to their exceptional picture-generating capabilities and extensive usage in data augmentation, Generative Adversarial Networks (GANs) have drawn interest in medical image processing. In [13], authors have focuses on three healthcare imaging modalities and organs, including cardiac cine-MRI, liver CT, and RGB retina pictures, we investigated several GAN designs, ranging from straightforward DCGAN to more complex style-based GANs. To assess the visual acuity of the pictures produced by GANs, their FID scores were computed using training data from well-known and frequently used datasets. By assessing the segmentation accuracy of a U-Net trained on these produced pictures and the original data, we further evaluated their use. The findings show that GANs are not created equal, with some doing poorly in applications involving medical imaging while others fared substantially better. The best GANs are able to produce medical pictures that are convincing by FID standards, pass certain criteria, and deceive skilled professionals in a visual Turing test. The findings of segmentation, however, imply that no GAN is able to replicate the complete richness of medical information.

Deep neural networks are now a beneficial technology for medical imaging workflow optimization and clinical care enhancement. So far, it has triggered a massive global interest and has gradually delivered promising outcomes when applied to multiple fields [14,15]. Deep learning's development in medical image analysis follows a slower but comparable path to computer vision. However, using computer vision techniques directly may not produce adequate results due to the differences between medical pictures and natural images. It is necessary to solve difficulties specific to medical imaging jobs in order to obtain optimal performance [16].

The hierarchical representation in Fig. 1 likely demonstrates how these trained DNN models can be applied to different stages of medical image analysis, starting from the raw input images and progressing towards more detailed and specific tasks. This hierarchical approach allows for the extraction of meaningful information from medical images and facilitates accurate and efficient pattern recognition.Let us now summarize the main DNN architectures reported in the literature in the context of medical image processing

2.1. Classification based on Convolutional Neural Networks (ConvNet/CNN)

This network structure was first described in [17] in 1989. Two essential parts of the CNN architecture are feature extractors and classification [18]. Convolution operations with different masks extract a

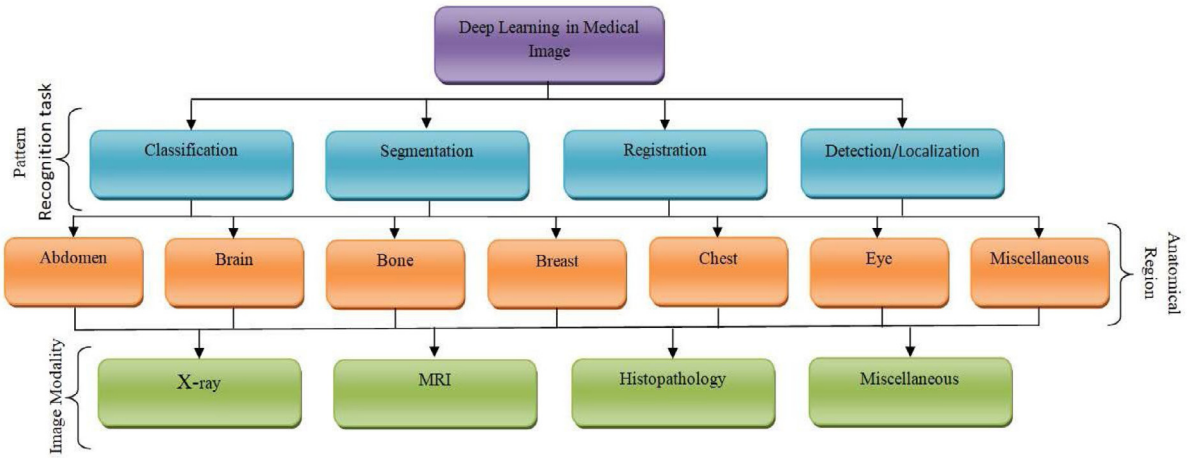

Fig. 1. Hierarchical representation of medical image analysis, in which neural networks have been applied.

set of features based on which classification is conducted. The ConvNet consists of three elementary types of layers: convolution, max-pooling, fully connected (FC), and softmax for classification.

Several essential processes are employed in convolutional neural networks (CNNs) for image classification, including convolution, max-pooling, fully connected (FC) layers, and softmax activation. Here is a description of each of these elements within the framework of CNN-based classification:

Convolution: The primary feature extraction algorithm used by CNNs is convolution. It entails applying to the input picture a collection of teachable filters, often known as kernels. Between its weights and the input's local receptive field, each filter performs a dot product. Edges, corners, and other little patterns or characteristics inside the image can be found with this technique. A series of feature maps, each of which reflects the response of a particular filter over the whole input picture, are the result of the convolutional layer.

Max-Pooling: Max-pooling is used to minimize the spatial dimensions and downsample the feature maps. Within each feature map, it acts on tiny rectangular sections (usually 2×2 or 3×3) and produces the greatest value therein. Max-pooling aids in preserving the most important aspects while removing unnecessary or duplicate information by choosing the maximum activation. Additionally, it adds a certain amount of translational invariance, strengthening the network's resistance to minute spatial fluctuations. Despite having smaller spatial dimensions, the resulting pooled feature maps nevertheless include vital details.

Softmax Activation: A softmax layer is often the last layer of the CNN and is utilized for classification. The previous FC layer's outputs are transformed into probabilities by Softmax. When the softmax function is used, the values are normalized and converted into a probability distribution. The softmax function makes sure that the probabilities add up to 1, and each output neuron belongs to a certain class. By choosing the class with the highest probability, the predicted class is established.

Convolutional layers are used by CNNs to extract local features, max-pooling layers to downsample and preserve important information, fully connected layers to capture global relationships, and a softmax activation layer for classification by supplying probability distributions over various classes. CNNs can successfully learn hierarchical representations from pictures and produce precise predictions because to this mix of activities.

Fig. 2 demonstrates the basic ConvNet architecture for the classification problem, which has been modified in terms of class numbers or/and layer types. Researchers further strengthened CNNs by increasing additional numbers of convolutional layers and other, for instance, dropout layers and published different state-of-the-art research work on various computer vision problems. For medical application details, see Section 4.

The significance of CNNs in disease detection lies in their ability to leverage the power of deep learning, extracting meaningful and discriminative features from medical images. By improving detection accuracy, reducing interpretation time, and providing consistent results, CNNs contribute to more effective and efficient disease diagnosis, enabling early intervention, better patient outcomes, and enhanced healthcare decision-making. This paper [20] gives an overview of the literature in the area of deep convolutional neural network-based medical picture segmentation. The article looks at a number of popular medical picture datasets, several segmentation task evaluation measures, and the effectiveness of various CNN-based networks. In [21] this article, authors have suggested a unique and computationally efficient deep learning strategy to exploit minimal data for learning domain invariant and generalizable representations in several medical imaging applications, such as malaria, diabetic retinopathy, and TB. The CNNs produced by our method are referred to as Incremental Modular Networks (IMNets), and we call our methodology Incremental Modular Network Synthesis (IMNS). Small network modules that we refer to as SubNets, which are capable of producing salient characteristics for a specific challenge, are the foundation of our IMNS strategy. Then, by merging these SubNets in various configurations, we create networks that are increasingly larger and more potent. Only one new SubNet module is subject to learning updates at each level. This facilitates network optimization and lowers the computing resource needs for training.

2.2. DNNs in segmentation based on U-NN and V-NN architecture

Deep neural networks (DNNs) have significantly advanced the field of medical image segmentation. Segmentation plays a crucial role in extracting precise information from medical images, such as identifying and delineating specific anatomical structures or pathological regions [22]. Here's how DNNs contribute to medical image segmentation:

Feature Learning: DNNs are capable of automatically learning complex and discriminative features directly from the input images. This eliminates the need for manual feature engineering and allows the network to adapt to different imaging modalities and anatomical variations [23]. Deep architectures, such as convolutional neural networks (CNNs), can capture both low-level features (e.g., edges, textures) and high-level semantic information (e.g., shapes, structures) through multiple layers of non-linear transformations. This feature learning ability enables DNNs to better represent the characteristics of medical images and improve segmentation accuracy [24].

End-to-End Learning: DNNs enable end-to-end learning, where the entire segmentation process is learned from the raw input images.

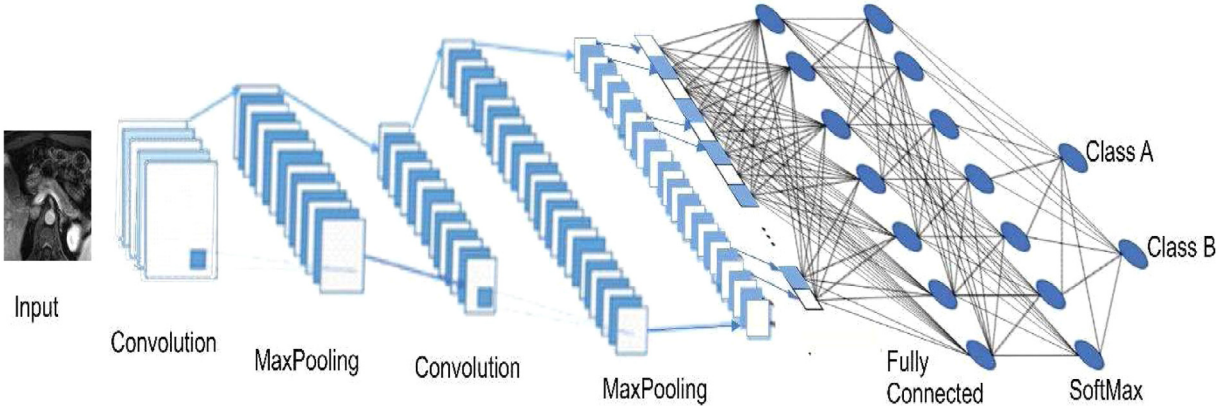

Fig. 2. CNN architecture for classification.

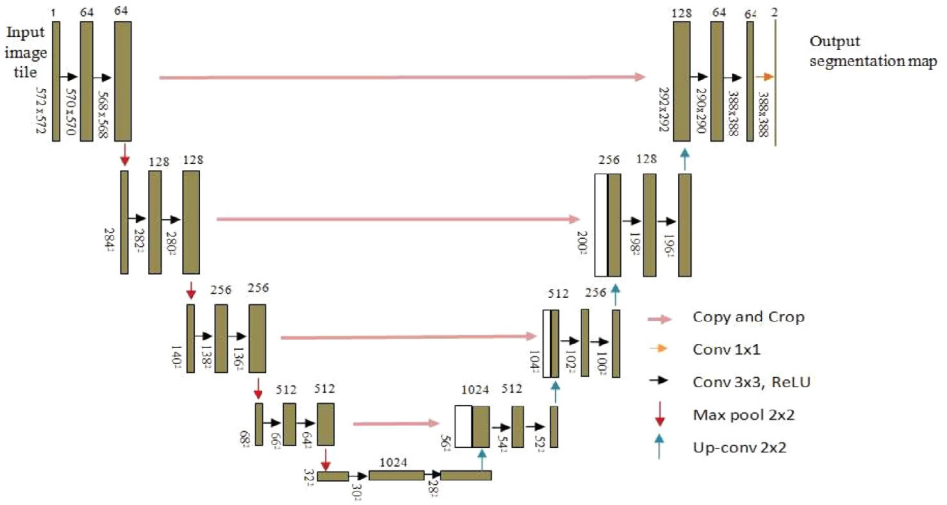

Fig. 3. U-Net DNN framework by [19]. Generally, the left half of this structure is called a decoder, and the right half of this structure is called an encoder.

Traditional segmentation methods often involve multi-step pipelines, including preprocessing, feature extraction, and classification [25]. DNNs, on the other hand, learn the segmentation task directly from the data. By optimizing the network parameters using labeled training data, DNNs can effectively learn to perform the segmentation task in a data-driven manner. This end-to-end learning approach simplifies the segmentation pipeline and can potentially yield better segmentation results.

Semantic Segmentation: DNNs, particularly CNNs, are widely used for semantic segmentation in medical imaging. Semantic segmentation aims to assign a label or class to each pixel or voxel in an image, effectively partitioning the image into different regions [26]. CNNs with fully convolutional architectures can process the entire image at once and generate dense pixel-wise predictions. The networks learn to associate image regions with specific classes during training, enabling accurate and detailed segmentation.

Training with Labeled Data: DNNs require large amounts of labeled data for training. Annotated medical image datasets are essential for training DNN-based segmentation models [27]. The availability of such datasets, along with advancements in data sharing and labeling efforts, has facilitated the development of robust and accurate segmentation models. However, labeled medical image datasets can still be limited or require extensive manual annotation, which remains a challenge in the field [28].

Post-processing Techniques: Post-processing techniques are often employed to refine and improve the segmentation results obtained from DNNs. These techniques may involve applying morphological operations, such as erosion or dilation, to remove small artifacts or smooth the segmented regions. Other methods may include region growing, graph-cut algorithms, or spatial regularization techniques to enforce consistency or incorporate prior knowledge. Post-processing can enhance the segmentation accuracy and improve the clinical usability of the results [29].

The U-Net architecture has become popular for medical image segmentation tasks. It consists of an encoder–decoder structure with skip connections [30]. The encoder path captures context and extracts features through convolution and pooling operations, while the decoder path recovers spatial resolution and refines the segmentation masks. Skip connections allow the network to combine low-level and high-level features, aiding in precise localization and preserving fine details [31]. U-Net and its variations have shown remarkable performance in various medical imaging segmentation challenges.

In this case, the network structure is symmetrical, consisting of an encoder–decoder framework, and it can be presented as a U-shape Network (U-Net) for 2D images or Volumetric Network (V-Net) [32] for 3D MRI images. Below, the conceptual layout of the U-net architecture depicts in Fig. 3. The set of layers is the same as in standard CNN, but their organization results in a segmented image, with the original resolution as the input one, where each pixel value is represented as belonging to a particular class [33].

Such an architecture is especially useful for medical image segmentation tasks. Here, in many cases, the tissues or organs are difficult to

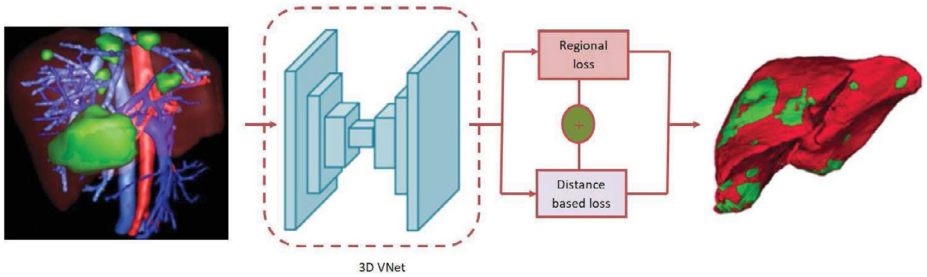

Fig. 4. An example of 3D organ visualization before an operation by means of a V-Net framework by [35].

Table 1
List of accessible datasets with an access link that exploits DNNs.

Application type	Modality	Dataset	Link
BreastCancer (BC)	Digital mammograms	DREAM [36]	https://www.synapse.org
BC	H&E stained	BreakHis [37]	https://web.inf.ufpr.br/
BC	H&E stained	MITOSTAPIA [38]	https://mitos-atypia-14.grand-challenge.org/
BC	H&E stained	BACH [39]	https://iciar2018-challenge.grand-challenge.org/
BC	H&E stained	CAMELYON16 [37]	https://camelyon16.grand-challenge.org/
BC	H&E stained	INBreast [40]	https://www.ncbi.nlm.nih.gov/pubmed/
BC	H&E stained	CAMELYON17 [41]	https://camelyon17.grand-challenge.org/
Chest X-ray (C X-ray)	X-ray	CheXperte [42]	https://stanfordmlgroup.github.io/competitions/
C X-ray	X-ray	MIMIC-CXR [43]	https://mimic-cxr.mit.edu/
Head And Neck (H & N)	CT images	PDDCA [44]	http://www.imagenglab.com/
H & N	PET scans	18F-FDG PET [45]	https://www.kaggle.com/c/pet-radiomics-challenges/
Lung Cancer (LC)	Low-Dose CT images	BOWL17 [46]	https://www.kaggle.com/c/data-science-bowl-2017/
LC	Computed Tomography (CT) scans	LIDC-IDRI [47]	https://wiki.cancerimagingarchive.net/
LungMask (LM)	CT Scan	LUMIC [48]	https://lumic.grand-challenge.org/
LungNode (LN)	CT Images	LUNA [49]	https://luna16.grand-challenge.org/
Mice LungLesions	H&E stained	ANH [50]	https://anhir.grand-challenge.org/
Mild traumatic brain injury	MRI	MTOP [51]	https://tbichallenge.wordpress.com/
Multimodal brain tumor segmentation	3T Multimodal MRI scans	BraTS 2018 [52]	https://www.med.upenn.edu/
Brain	3T MRI Scans	MRBrainS18 [53]	https://mrbrains18.isi.uu.nl/
Brain	CT-MR And PET-MR	RIRE [54]	http://insight-journal.org/
Brain	MRI	MUSHAC [55]	https://projects.iq.harvard.edu/
Brain tumor	MRI	Curiou [56]	https://curious2018.grand-challenge.org/
Alzheimer'sDiseaseNeuroimagingInitiative	MR And PET	TADPOLE [57]	https://tadpole.grand-challenge.org/
DiabeticRetinopathy	FundusImages	IDRID [58]	https://idrid.grand-challenge.org/
Digital RetinalVessel extraction	Non-Mydriatic 3CCD Camera	DRIVE [59]	https://drive.grand-challenge.org/ [60]
Retinal OCT fluid	OCT Scan	RETOU [61]	https://retouch.grand-challenge.org
CardiacDiagnosis	MRI	ACDC17 [62]	https://www.creatis.insa-lyon.fr/
Cardiac	ECG	ECG Arrhythmia [63]	https://irhythm.github.io/cardiol_test_set/
Pulmonary angiograms	CT scans	CAD-PE [64]	http://www.cad-pe.org
Liver	Ultrasound	CLUST [65]	https://clust.ethz.ch/
Abdominal	CT And MRI	CHAOS [66]	https://chaos.grand-challenge.org/Data/
KidneyCancer	CT	KITS [67]	https://kits19.grand-challenge.org/data/
GastroenterologicalDiseases	Endoscopy	AIDA [68]	https://isbi-aida.grand-challenge.org/
X-ray Normal/Abnormal detection.	X-ray	MURA [69]	https://stanfordmlgroup.github.io/
Low back pain	MRI	IVDM3S [70]	https://ivdm3seg.weebly.com/
Child age prediction	X-ray	Rsna-bone-age [71]	https://www.kaggle.com/
Knee	MRI	MRNet-v1.0 [72]	https://stanfordmlgroup.github.io/
Automatic vertebral fracture analysis and identification	X-ray	VFA, DXA [73]	http://spineweb.digitalimaginggroup.ca/
Tumors	H&E stained	Warwick-QU [74]	https://warwick.ac.uk/
Skin cancer	Dermo.S.	ISIC [75]	https://challenge2019.isic-archive.com/
Skin cancer	Dermo.S	Skin cancer MNIST [76]	https://www.kaggle.com/

recognize in the unprocessed image, even for a professional. Whereas, after segmentation, they become easily noticeable [34].

The network designers have gone even further and attempted to segment the diseased organs in 3D for better visualization, especially when an operation (invasive medical procedure) is necessary. The best example of such an approach is the 3D V-net architecture, which was recently proposed by Ronneberger, Fischer, & Brox in [35]. The authors proposed a 3D liver segmentation and tumor identification technique based on a 3D V-Net, which is shown in Fig. 4. Here, input images came from two datasets, LiTS [77] and 3D-IRCADb (see Table 1). In [78] this work, authors have introduce a novel region-to-boundary deep learning model to provide a practical solution to this problem. Authors have initially use a U-shaped network with two branches below the final layer to build the target probability map and the associated signed distance map. Second, using the signed distance map and collected multi-scale features, we focus on the boundary of the target lesions or organs that need to be segmented. The results are then obtained by combining the border and region properties. In [79] authors have suggest Axial Fusion Transformer UNet (AFTer-UNet), which combines the strengths of transformers for long sequence modeling with convolutional layers' capacity to extract fine-grained data. It uses long-range signals from inside and between slices to direct segmentation. Compared to the earlier transformer-based models, it trains faster and uses fewer parameters. Extensive tests on three multi-organ segmentation datasets show that our method performs better than the most recent state-of-the-art approaches.

This architecture has many variations, including the DENSE-INception U-net, among others [80]. This solution has been tested on different organ images, for instance, lungs segmentation of CT data obtaining an average Dice score of 98.57%, blood vessel segmentation

obtaining an average Dice score of 95.82%, and MRI scan brain tumor segmentation with an average Dice-score 98.67%.

2.3. DNN architecture for object detection

Deep neural networks (DNNs) have had a profound impact on object detection, which involves locating and classifying objects within images or videos. The significance of DNNs for object detection can be understood through the following key points:

Accuracy: DNNs have demonstrated exceptional accuracy in object detection tasks. Through the use of deep architectures, such as convolutional neural networks (CNNs), DNNs can learn complex and discriminative features from images, enabling precise object localization and classification [81]. The hierarchical nature of DNNs allows for the extraction of features at multiple scales and levels of abstraction, capturing both local and global information. This leads to highly accurate object detection results, outperforming traditional methods.

End-to-End Learning: DNNs facilitate end-to-end learning, where the entire object detection pipeline can be learned directly from the data. Traditional object detection methods often involve multiple stages, including feature extraction, region proposal generation, and classification. DNNs, on the other hand, can learn to perform all these steps simultaneously within a single network. This end-to-end learning approach reduces complexity, eliminates the need for handcrafted features, and optimizes the entire detection process, resulting in improved accuracy and efficiency [82].

Flexibility and Adaptability: DNNs offer flexibility and adaptability to various object detection scenarios. They can detect objects across different classes, sizes, orientations, and scales. The training process of DNNs involves optimizing the network parameters using labeled datasets, allowing them to learn the specific characteristics of objects within a given domain. This adaptability makes DNNs suitable for a wide range of applications, from detecting everyday objects in images to specialized tasks like detecting specific anatomical structures in medical imaging [83].

Real-Time Performance: DNNs have made real-time object detection possible. With advancements in hardware, optimization techniques, and model architectures, DNN-based object detection can achieve high frame rates, enabling applications in real-time video analysis, autonomous driving, surveillance, and robotics. Techniques like single-shot detectors (SSDs) and region-based convolutional neural networks (R-CNNs) have been developed to balance accuracy and speed, making DNN-based object detection practical for real-world applications [84].

Transfer Learning and Pre-trained Models: DNNs facilitate transfer learning, where models trained on large-scale datasets can be fine-tuned for specific object detection tasks with limited training data. Pre-trained models, trained on massive datasets like ImageNet, serve as a starting point, allowing users to leverage the knowledge and feature representations learned from these datasets. This significantly reduces the amount of data and computation required to train object detection models from scratch, making it more accessible and feasible for various applications [85].

Rich Contextual Information: DNNs can effectively utilize rich contextual information for object detection. By learning from large-scale datasets, DNNs can capture and understand the contextual relationships between objects and their surrounding environment. This contextual understanding improves the accuracy of object detection by incorporating contextual cues, spatial relationships, and semantic information. For example, DNNs can exploit the context of object co-occurrences, object shapes, or scene context to improve the detection and reduce false positives.

DNNs have revolutionized object detection by significantly improving accuracy, enabling end-to-end learning, offering flexibility, achieving real-time performance, supporting transfer learning, and leveraging rich contextual information. These advancements have made DNN-based object detection a critical technology in various fields, including computer vision, autonomous systems, robotics, surveillance, and beyond.

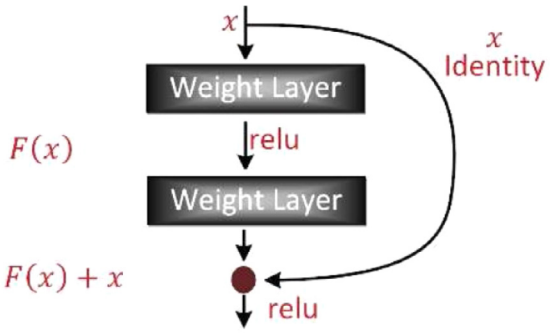

Fig. 5. The conceptual layout of Faster R-CNN architecture [88].

The GenPSOWVQ approach [86], a novel wavelet-based recurrent neural network technique for image reduction. Combining genetic algorithms and fragments, the codebook is created. When encoding clinical pictures, the recently developed image compression model achieves exact compression while retaining image accuracy with lower computing costs. Real-time medical imaging was used to test the suggested technique utilizing PSNR, MSE, SSIM, NMSE, SNR, and CR indicators. [87] author have suggest the Mixed Transformer Module (MTM), a brand-new Transformer module for simultaneous learning of intra- and inter-affinities. First, MTM efficiently determines self-affinities using our clever Local–Global Gaussian-Weighted Self-Attention (LGG-SA). Then, it uses External Attention (EA) to mine links between data samples. We create the Mixed Transformer U-Net (MT-UNet) model for precise medical picture segmentation using MTM. The experimental findings demonstrate that the suggested technique outperforms existing state-of-the-art methods on two separate public datasets where tested.

Last but not least, DNN architecture can be used for object detection. In this case, two network functions are used: classification and spatial location. These functions can be obtained thanks to the Residual Networks, consisting of many similar modules, e.g., RezNet-50 or RezNet-101 [88]. One such module is illustrated in Fig. 5. The main flow is responsible for object classification, whereas the feedforward is responsible for the transfer of spatial location information.

In medical imaging, R-CNN can be used to detect objects, for instance, in X-ray images [89]. This architecture can even be applied in a real-time segmentation technique, which is presented by the authors [90], who used it in a prostate biopsy procedure.

We propose anEnhance-NetDLM approach to improve the performance of musculoskeletal radiographs X-ray images. The highlight of this research is to assess the impact of three different image enhancement techniques (CLAHE, HEF, and UM) on green channel grayscale the medical musculoskeletal radiographs X-ray images for DLMs. The paper is organized into six different sections as follows: the most crucial related works are described in the second section. In the third section, we have discussed the materials and methods used for the proposed model. In the fourth section, we have elaborated on the proposed model. In the fifth section, we have explained the simulation, results, and validation in detail. In the last section, we have discussed the conclusion and future scope.

3. Medical image datasets organized according to organs

Neural networks (regardless of their architecture) need data for training. Let us summarize most of the publicly available medical imaging data sets according to the pattern recognition tasks in the context in which they have been applied. The process of neural training

requires a big training set. In the case of medical imaging, several problems arise frequently; therefore, an important contribution of this article is putting together and subjecting to critical analysis the medical image sets divided into organs and image modalities. The research was carried out in different anatomical regions to support medical practitioners. Table 1 lists accessible datasets that can be used for DNN training. In addition to the link to the actual data set, information about the specific modality that is represented is provided. This article [91] covers a machine learning and image processing-based evolutionary method for categorizing and identifying breast cancer. To assist in the classification and detection of skin disorders, this model integrates image preprocessing, feature extraction, feature selection, and machine learning approaches. The geometric mean filter is applied to improve the quality of the image. Features are extracted using AlexNet. The relief algorithm is used to pick features. The model uses machine learning methods such least square support vector machine, KNN, random forest, and Nave Bayes for illness classification and detection. Data gathering from MIAS is utilized in the experimental inquiry. Using image analysis to correctly diagnose breast cancer illness is a benefit of the suggested method.

The collected datasets were selected by clinical experts and manually prepared from the most interesting point of medical view. Databases include several sets of anonymized medical images of patients. Some of the above datasets have been goals of different challenges organized to evaluate new and existing algorithms for automated classification, detection, or segmentation in order to reduce the time required to diagnose a patient.

Transfer Learning (TL) architectures for automated medical image processing. Authors have revealed that TL has been used for a variety of medical imaging applications, including segmentation, object recognition, illness classification, and severity grading, to mention a few [92]. We could prove that TL uses less training data than conventional deep learning techniques while still offering high-quality decision assistance. The fact that TL models have previously been trained on sizable generic datasets and that a task-specific dataset is merely utilized to customize the model gives birth to these favorable qualities.

For a medical purpose, information not only from pure images or one modality is used. Additionally, the process of image registration, which is aligning two or more images, has had to be employed. In (semi-)automatic medical image analysis, it is a well-established approach for transferring information across pictures. Methods for registering images based on picture intensity and characteristics that are manually constructed are among the most common. Images may now be registered with the use of supervised and unsupervised deep learning algorithms in recent years [93,94].

4. DNN applications using medical imaging datasets

With knowledge of main NN architectures and popular datasets that can be used for their training, let us now summarize recent developments and research work carried out in the different anatomical regions.

The primary goal of this part is to demonstrate how and where publicly accessible medical imaging data sets are utilized in the area of DNN architectures described in Section 2. The research was carried out in the different anatomical regions, such as the kidney, liver, brain, breast, chest, eye, etc., to support medical practitioners.

4.1. DNNapplications in lung diseases

In this subsection, we present some examples of the above-mentioned DNN techniques in lung diseases. Before the COVID-19 pandemic, the first attempts were made for diagnoses lung diseases based on CT images. Abdelhamid et al. [95] implemented the U-Net model, trained as an end-to-end model with a performance of 95.02% of the Dice-Coefficient index.

In some cases, the image registration turned out to be a problem. Berendsen et al. [93] implemented a ConvNet-based model for 3D image registration, and after limited training, the average registration time was as good as 0.63 s for multistage image registration.

Ferreira et al. [96] suggested a V-Net model for segmentation tasks that was fully regularized. It implements regularization techniques, such as dropout, multi-task learning, deep-supervision, and batch normalization. The model performs an average per-lobe Dice Coefficient of 93.6% and an inter-lobar Dice Coefficient of 76.2%.

The outbreak of the COVID-19 pandemic resulted in an urgent necessity for fast respiratory tract diagnosis in case of pneumonia and other lung infections. Oh, Park and Ye [97] implemented a combination of FC-DenseNet-103 for segmentation and ResNet-18 for classification. An accuracy rate of 88.9 percent was reached by the model. Ucaret al. [98] suggested a deep Bayes-Squeeze Net model (convolutional network with Bayesian optimization) diagnose COVID-19. The proposed approach solves the dataset imbalance issue and implements a multiscale offline augmentation. The experiment reported shows an accuracy of 98.26%.

Wu et al. [99] proposed a deep multi-view deep learning fusion model to diagnose COVID-19. Based on the modified ResNet-50 and the experiment shows an accuracy of 76.0%. Behzadi-Khormouji et al. [100] implemented a three-phase pre-processing method to improve the DNN model, referred to as ChestNet. The experiment achieved an accuracy of 94.67%. Mittal et al. [101] implemented two models for the integration of convolutions with capsules (ICC) and an ensemble of convolutions with capsules (ECC) and achieved an accuracy of 95.33% and 95.90%, respectively. As defined by the Neuronal Activity Vector (NAV), a capsule is a small collection of neurons whose activity vector indicates the precise parameters of an entity of a given kind, such as a component of an item or the object itself, introduced by Sabour, Frosst, & Hinton [102].

Chest X-rays are used to see how much virus is in the lungs in different sections of the body. Chest radiographs are the preferred method of diagnosis since laboratory testing takes a long time and requires a great deal of human work. It is possible to determine if a patient is suffering from viral-pneumonia, COVID-19, or has a normal profile by looking at their chest X-ray scans [103]. For binary classification, their model was 99.48% accurate, while for three-class classification, it was 97% accurate.

Overall, researchers have successfully trained different DNN architectures for the classification, detection, registration, and segmentation of lung disease with high accuracy [104]. Table 2 summarizes the above-mentioned approaches and results in the most compact way.

4.2. DNN applications for eye diseases

DNN has also been applied in ophthalmology at the same time as for the diagnostics of other organs, e.g., to retinal fundus images for the classification of diabetic retinopathy; predicting age and gender, retinopathy, macular edema, glaucoma-like disk. Nagasato et al. [105] implemented the Visual Geometry Group VGG-16 model [106]. The analysis showed an AUC of 98.6%.

Wu, Xia et al. [107] proposed the NFN+ model, which contains two cascaded, identical multiscale structures for preparing a retinal vessel map. Each segmented network framework has an encoder–decoder architecture with 3×3 Conv-ReLU layers (compare Fig. 3). The model achieved AUC for three different datasets, DRIVE, STARE, and CHASE (see Table 1 for characteristics of the DRIVE dataset) of 98.30%, 98.75%, and 98.94%, respectively.

Riaz et al. [108] proposed a multiclass, deep, and densely connected model. There, the EyePACS dataset was used for the experiment. The analysis showed an average F1score of 97.0%. Liu et al. [109] implemented a self-adaptive deep learning method based on Inception-V3, and the analysis showed an AUC of 99.50%. Zhang et al. [80]

Table 2
Summary of DNN techniques for lung diseases.

Reference	Studied	Task	Modality	Architecture/Layers	Result
Oh Park and Ye [97]	COVID-19	Detection	X-ray	Combination of FC-DenseNet103 and ResNet18	Accuracy 88.9%
Ucar and Korkmaz [98]	COVID-19	Detection	X-ray	Deep Bayes-SqueezeNet	Accuracy 98.26%
Wu et al. [99]	COVID-19	Detection	CT	Multi-view deep learning fusion model	Accuracy, 76.0%
Abdelhamid et al. [95]	Lung	Segmentation	X-ray	Unet	Model performance 0.9502 Dice-Coefficient index
Berendsen et al. [93]	Lung	Registration	X-ray	Deep Learning Image Registration	The average registration time for multistage image registration was 0.63 s.
Ferreira et al. [96]	LungLobe	Segmentation	3D CT	V-Net	The model performs an il-DC Coefficient of 76.2% and an average pl-DC of 93.6%.
Mittal et al. [101]	Pneumonia	Detection	X-ray	ICC and ECC	Achieved accuracy of 95.33% and 95.90%, respectively
Behzadi-Khormouji et al. [100]	Respiratory disease	Detection	X-ray	ChestNet	Model accuracy 94.67%

Table 3
Summary of DNN techniques for eye diseases.

Reference	Studied	Application	Architecture/Layers	Modality	Result
Nagasato et al. [105]	Detect a nonperfusion area (NPA)	Classification	VGG-16 model	Optical coherence tomography angiography (OCTA) images	AUC 98.6%
Wu, Xia et al. [107]	DiabeticRetinopathy	Segmentation	NFN+ Model	FundusRetinal image	AUC DRIVE, STARE, CHASE 98.30%, 98.75%, 98.94% respectively
Riaz et al. [108]	DiabeticRetinopathy	Classification	Multiclass deep and densely connected mode	Fundus-Retinal image	Average F1-score AUC97.0%.
Zhang et al. [80]	Blood vessel segmentation, Lung's segmentation, and Brain tumor segmentation	Segmentation	Seg-Net, FCN-8s, U-Net, U-Net, DIU-Net-1, DIU-Net	CT, Fundus-Retinal image, MRI	Average-Dice-Score of 0.9867

model combine the inception unit with dense connections in the U-Net framework. The experiment showed an Average Dice score of 98.67%.

Kim et al. [110] implemented the CNN model trained using retinal fundus images age prediction. The model achieved MAE of 3.06 on the test set of 24,366 images.

The summary of the DNN technique for ophthalmology classification, segmentation, detection, and prediction using different image modalities is shown in Table 3. Overall, these researches cover the retinopathy resulting from different causes and diagnosed based on various imaging.

4.3. DNN applications for bone age diseases

The skeleton or bone age automatic evaluation is a very new subject for deep learning. So far, visual assessment of boneage, based on a solitary reference X-ray image, has been the standard, and due to the fact that such assessment is a time-limited process, it is subject to the variability of interpretations.

Most of the ongoing research focuses on designing a novel approach to predict boneage, using left-hand radiology images for a child. C. Spampinato et al. [111] proposed a two-stage DNN model, a first-stage CNN network for automatic feature extraction, and a second-stage regression model for bone-age prediction. They obtained an average evaluation discrepancy of about 0.8 years.

H. Lee et al. [112] performed a study based on 8325 images and proposed a data-driven CNN transfer learning for automatic feature extraction. Their model has accomplished an accuracy of 57.32% and 61.40% for both gender, females and male, respectively. Larson et al. [113] performed a study based on 14 036 images and implemented ResNet-50 architecture. The analysis showed validation and test accuracies of 66.2% and 49.7%, respectively.

S. S. Halabi et al. [71] performed a study concerning pediatric boneage based on 14 236 images and implemented Inception V3, ResNet-50, Ice Module Architecture, ML using handcrafted features and Gabor texture energies, U-Net. The analysis results, based on a mean absolute distance (MAD), revealed 4.2, 4.4, 4.4, 4.5, and 4.5 months, respectively.

S. Koitka et al. [114] implemented an Inception-ResNet-V2 model. The analysis showed the average F1-Score to be 91.85%.

S. H. Tajmir et al. [115] focused on building a CNN model based on LeNet-5 introduced in 1989 by Yann LeCun [116], with a stride of 4 and image patch size 32×32, for bone age assessment (BAA) as a tool in the calculation of metabolic disorders and pediatric endocrine. Bone-age assessment performance was found to be 68.2 percent accurate overall and 98.6 percent within a year of the model.

V. I. Iglovikov et al. [117] performed a study on 12,600 radiological images and implemented VGG-style DNN 6 convolutional layers followed by two fully connected blocks. There was a mean absolute error of 4.97 months in the procedure.J. C. Castillo et al. [118] performed the study on 14 949 radiological images and implemented VGG16. Patients of both genders, male and female, had an MAE of 9.82/10.75 months when using the CNN design.

T. Van Steenkiste et al. [119] performed the study based on 12 611 radiograph images of children from the age group of 0 to 19 years. The Gaussian process regression was applied to aggregate results obtained from the augmented DNN model, which yielded an accuracy rate of 94.45% and a mean spread of 6.80 months inside a year.

Transfer learning was examined by Kandel et al. [120] for its impact on the classification of musculoskeletal pictures. After analyzing the 168 results acquired utilizing six different architectures for CNNs and seven distinct kinds of bones, the scientists discovered that the transfer

Table 4
Summary of DNN techniques for bone age prediction using X-ray image modality.

Reference	Dataset size	Architecture/Layers	Result
C. Spampinato et al. [111]	1391	BoNet architecture.	The average discrepancy is about 0.8 years.
H. Lee et al. [121]	8325	CNN-based pre-processing engine images.	Fine-tuned CNN accuracies of 57.32% and 61.40% for females and males.
D. Larson et al. [114]	14 236	ResNet-50	Testand validation accuracies are 0.497 and 0.662, respectively.
S. S. Halabi et al. [71]	14 236	Inception V3, ResNet- 50, Ice Module Architecture, ML using handcrafted features and Gabor texture energies, U-Net.	Using MAD, the best five outcomes were 4.2, 4.4, 4.4, 4.5, and 4.5 months, respectively.
S. Koitka et al. [114]	14 236	Inception-ResNet-V2	F1-Score on average, 91.85%.
S. H. Tajmir et al. [115]	1681	LeNet-5	According to the results mean six-reader cohort accuracy was 63.6 percent overall and 97.4 percent within one year.
V. I. Iglovikov et al. [117]	12 600	VGG-style CNN	The method achieved a mean absolute error (MAE) equal to 4.97 months.
J. C. Castillo et al. [118]	14 949	VGG-16	Patients of both genders, male and female, had an MAE of 9.82/10.75 months when using the CNN design.
T. Van Steenkiste et al. [122]	14 236	VGG-16	The method has a 94.45 percent accuracy rate and a mean range of 6.80 months after one year.
Kandel et al. [120]	Training: normal 21,935 fractured 14,873 Test: normal 1667 fractured 1530	Wrist: DenseNet, Finger: InceptionResNetV2, Elbow: Xception, Forearm: DenseNet121, Humerus: VGG-19, Hand: Xception, Shoulder: Xception.	The overall accuracy of different models oscillated from 70% to 80%, which is compared to radiologists' results.

learning approach outperformed training a CNN from scratch in terms of accuracy.

The summary of the DNN technique for bone age prediction using X-ray image modality is shown in Table 4. Our summary covers the research concerning bone age for all age groups, from children to old people.

4.4. DNN applications for osteosarcoma diagnostics

Digital automation in the area of histopathology is restricted because of the intricacy of tissue structure. Osteoblasts, osteocytes, and osteoclasts serve as a visual representation of the various tissue types seen in a typical bone biopsy sample. The malignant characteristics of these cells include nuclear membrane abnormalities, pleomorphism, large multinucleated cells, hyperchromatic nuclei, and aberrant mitosis.

Hematoxylin and eosin (H&E) stained datasets of cancer cells on a histology slide are used in the majority of cancer research. H&E staining dyes the nuclei blue and the background tissues pink, and it is used in the majority of cancer research. The slide preparation and incorrect staining reaction have an impact on the digital picture quality, which may result in numerous cellular areas and tissues being under-represented in the digital image.

R. Mishra et al. [123] designed a CNN, which concentrated on a training phase of categorization into three classes: live tumor, necrosis, and non-tumor. Assigning tumor classifications is accomplished by using the trained classifier as a sliding window on top of the collected data. Because CNN works on raw pixel data, there is no need for human input. A noteworthy benefit over earlier efforts, apart from the initial annotation of slides for the training data, was the attainment of classification accuracy of roughly 84 percent, which was a substantial improvement over past attempts.

O. Daescu et al. [124] performed a study on 64,000 osteosarcoma image patches, resized to 128 × 128, and proposed a CNN model, which achieved a classification accuracy of around 92.4%. In [125] description of explainable artificial intelligence (XAI), which is applied to medical picture analysis using deep learning. For the purpose of categorizing deep learning-based medical image analysis techniques, a framework of XAI criteria is presented. The papers are then surveyed and categorized in accordance with the framework and according to anatomical location for use in medical image analysis. In [126] this study, we propose a hybrid artificial intelligence (AI) framework to identify major chronic risk factors of novel, contagious diseases as early as possible at the time of pandemics. The proposed framework combines evolutionary search algorithms with machine learning and the novel explanatory AI (XAI) methods to detect the most critical risk factors, use them to predict patients at high risk of mortality, and analyze the risk factors at the individual level for each high-risk patient.

H. B. Arunachalam et al. [127] focused on fine-tuning hyper parameters, based on gradient descent, with a learning rate of 10-3 and a batch size of 100. The model was run for 20 epochs and achieved 93% of accuracy. M. D Acunto et al. [128] implemented a Faster R- CNN model. The analysis showed an accuracy of 97%.

The summary of the DNN technique for osteosarcoma cell detection and classification using H&E image modality is shown in Table 5. Because of structural complexity and difficulties in recognition between normal and disease cells, there have been many architectures tested with relatively small size data sets.

5. ChallengesandFutureDirections

This paper summarizes how deep neural networks can help the doctor determine a clinical situation. As it has been shown, DNN-based approaches produce low false-positive levels and speed up the decision process. It has been demonstrated that different deep learning algorithms offer greater accuracy in the field of medical imaging than human expert evaluation.

The remote hospital, especially in the COVID-19 era, should offer considerable assistance not only to patients but also to doctors. In order to achieve the aim of health for all, virtual hospitals should offer the same degree of diagnostic sophistication to an individual in a rural community as well as to an urban one, generally independently of the geographic location of the patient. In the future, virtual hospitals, thanks to a robust computer infrastructure applying DNNs to image processing, will help to build a remote healthcare system.

Representative datasets have played a critical role in the advancement of research and innovation in a wide range of high-profile areas of data science, including computer vision. In the process of monitoring an ongoing disease, the development of medical imaging is essential. MRI, CT scans, and other medical modalities allow the doctor to track the treatment effectiveness and change procedures where it is

Table 5
Summary of DNN technique for osteosarcoma cell detection and classification using H&E-stained image modality.

Reference	Osteosarcoma studied	Dataset size	Architecture/Techniques	Result
R. Mishra et al. [123]	Viable and non-viable tumor prediction	5000	AlexNet, LeNet, VGGNet, and Proposed architecture	AlexNet: 0.73, LeNet: 0.67, and Proposed architecture: 0.84
O. Daescu et al. [127]	Histopathological analysis of osteosarcoma	64,000	AlexNet, LeNet, VGGNet, Baseline architecture, and Proposed architecture	The overall accuracy of different models AlexNet: 0.78, LeNet: 0.71, and Proposed architecture: 0.867
H. B. Arunachalam et al. [129]	Human osteosarcoma cell detection and classification	942	Decision trees, SVM, Ensemble learning, and CNN	The overall accuracy of different techniques: Decision trees, SVM, Ensemble learning, and CNN achieves 80.9%, 89.9%, 86.6%, and 93%.
M. DAcunto et al. [128]	Human osteosarcoma cell detection and classification	48	Faster R-CNN	The accuracy is 0.97.

appropriate. The detailed knowledge provided by 3D medical imaging offers more thorough treatment for the patients. This high precision obtained thanks to 3D CNNs is used for medical image diagnosis.

6. Conclusion

This article presents a comprehensive overview of the recent developments in the area of deep learning concerning the diagnosis process. It focuses on organ diseases, such as kidney, liver, breast, brain, chest, eye, bone fracture, bone age prediction, and osteosarcoma based on medical imaging. It covers four primary directions.

In the first section, the background to DNN development in medical imaging is outlined. The second section provides an overview of the basic DNN architectures and a case study of the top DNN frameworks. Ongoing research in this sector, such as CNNs, has been successfully implemented in medical image classification, V-Nets in segmentation, and ResNet in detection. The 3D V-Nets are complex neural systems used in recent times to examine clinical data. The third section elaborates on article contributions to the open-source datasets which can be used in medical image analysis.

In the fourth section, the article focuses on the research work done in the field of deep learning in order to assist the healthcare worker in offering treatment for diseases. Materials are divided according to the organs. The authors have discussed multiple deep learning frameworks for medical imaging and the prospects for their applications, especially for the machine learning and computer vision community, to solve medical imaging tasks. The goal of a lot of ongoing research is to aid medical professionals by developing automated systems to examine images and identify acute disorders including brain tumors, bone cancer, breast cancer, bone fracture, and many more. This thorough analysis provides a summary of current developments in deep neural network-based medical imaging. In addition to the thorough literature evaluation, a list of publicly accessible data sources and potential future study areas are outlined. In the future, medical communities and patients will benefit from addressing challenges related to diagnosing critical diseases. Deep learning models can analyze medical images in conjunction with other clinical data, such as genomics or electronic health records, to enable personalized medicine. By integrating patient-specific information, DNNs can assist in treatment planning, prognostication, and selection of optimal therapies based on image-derived features and patterns.

Declaration of competing interest

The authors declare that they have no known competing financial interests or personal relationships that could have appeared to influence the work reported in this paper.

Data availability

Data will be made available on request.

References

[1] J.L. McClelland, D.E. Rumelhart, P.D.P.R. Group, et al., Parallel Distributed Processing, Vol. 2, MIT Press, Cambridge, MA, 1986.

[2] S. Suganyadevi, V. Seethalakshmi, K. Balasamy, A review on deep learning in medical image analysis, Int. J. Multimed. Inf. Retr. 11 (1) (2022) 19–38.

[3] V. Chang, V.R. Bhavani, A.Q. Xu, M.A. Hossain, An artificial intelligence model for heart disease detection using machine learning algorithms, Healthc. Anal. 2 (2022) 100016.

[4] M. Izadikhah, A fuzzy stochastic slacks-based data envelopment analysis model with application to healthcare efficiency, Healthc. Anal. 2 (2022) 100038.

[5] M.K. Rohil, V. Magotra, An exploratory study of automatic text summarization in biomedical and healthcare domain, Healthc. Anal. 2 (2022) 100058.

[6] M.S. Pathan, A. Nag, M.M. Pathan, S. Dev, Analyzing the impact of feature selection on the accuracy of heart disease prediction, Healthc. Anal. 2 (2022) 100060.

[7] G. Huang, Y. Sun, Z. Liu, D. Sedra, K.Q. Weinberger, Deep networks with stochastic depth, in: European Conference on Computer Vision, 2016, pp. 646–661.

[8] C. Nwankpa, W. Ijomah, A. Gachagan, S. Marshall, Activation functions: Comparison of trends in practice and research for deep learning, 2018, pp. 1–20.

[9] M.F. Kabir, T. Chen, S.A. Ludwig, A performance analysis of dimensionality reduction algorithms in machine learning models for cancer prediction, Healthc. Anal. 3 (2023) 100125.

[10] F. Masood, M. Driss, W. Boulila, J. Ahmad, S.U. Rehman, S.U. Jan, A. Qayyum, W.J. Buchanan, A lightweight chaos-based medical image encryption scheme using random shuffling and XOR operations, Wirel. Pers. Commun. 127 (2) (2022) 1405–1432.

[11] B. Davazdahemami, P. Peng, D. Delen, A deep learning approach for predicting early bounce-backs to the emergency departments, Healthc. Anal. 2 (2022) 100018.

[12] Y. Chen, X.-H. Yang, Z. Wei, A.A. Heidari, N. Zheng, Z. Li, H. Chen, H. Hu, Q. Zhou, Q. Guan, Generative adversarial networks in medical image augmentation: A review, Comput. Biol. Med. 144 (2022) 105382.

[13] Y. Skandarani, P.-M. Jodoin, A. Lalande, GANs for medical image synthesis: An empirical study, J. Imaging 9 (3) (2023).

[14] J. Cheng, S. Tian, L. Yu, C. Gao, X. Kang, X. Ma, W. Wu, S. Liu, H. Lu, ResGANet: Residual group attention network for medical image classification and segmentation, Med. Image Anal. 76 (2022) 102313.

[15] Q. Guan, Y. Chen, Z. Wei, A.A. Heidari, H. Hu, X.-H. Yang, J. Zheng, Q. Zhou, H. Chen, F. Chen, Medical image augmentation for lesion detection using a texture-constrained multichannel progressive GAN, Comput. Biol. Med. 145 (2022) 105444.

[16] X. Chen, X. Wang, K. Zhang, K.-M. Fung, T.C. Thai, K. Moore, R.S. Mannel, H. Liu, B. Zheng, Y. Qiu, Recent advances and clinical applications of deep learning in medical image analysis, Med. Image Anal. 79 (2022) 102444.

[17] K. Fukushima, Neocognitron: A hierarchical neural network capable of visual pattern recognition, Neural Netw. 1 (2) (1988) 119–130.

[18] A. Krizhevsky, I. Sutskever, G.E. Hinton, Imagenet classification with deep convolutional neural networks, Adv. Neural Inf. Process. Syst. 25 (2012) 1097–1105.

[19] O. Ronneberger, P. Fischer, T. Brox, U-net: Convolutional networks for biomedical image segmentation, in: International Conference on Medical Image Computing and Computer-Assisted Intervention, 2015, pp. 234–241.

[20] P. Malhotra, S. Gupta, D. Koundal, A. Zaguia, W. Enbeyle, Deep neural networks for medical image segmentation, J. Healthc. Eng. 2022 (2022) 9580991.

[21] R. Ali, R.C. Hardie, B.N. Narayanan, T.M. Kebede, IMNets: Deep learning using an incremental modular network synthesis approach for medical imaging applications, Appl. Sci. 12 (11) (2022).

[22] X. Xie, X. Pan, W. Zhang, J. An, A context hierarchical integrated network for medical image segmentation, Comput. Electr. Eng. 101 (2022) 108029.

[23] P.R. Jeyaraj, E.R.S. Nadar, Medical image annotation and classification employing pyramidal feature specific lightweight deep convolution neural network, Comput. Methods Biomech. Biomed. Eng. Imaging Vis. (2023) 1–12.

[24] T. Zhou, L. Li, G. Bredell, J. Li, J. Unkelbach, E. Konukoglu, Volumetric memory network for interactive medical image segmentation, Med. Image Anal. 83 (2023) 102599.

[25] L. Xie, L.E.M. Wisse, J. Wang, S. Ravikumar, P. Khandelwal, T. Glenn, A. Luther, S. Lim, D.A. Wolk, P.A. Yushkevich, Deep label fusion: A generalizable hybrid multi-atlas and deep convolutional neural network for medical image segmentation, Med. Image Anal. 83 (2023) 102683.

[26] X. Xie, W. Zhang, X. Pan, L. Xie, F. Shao, W. Zhao, J. An, CANet: Context aware network with dual-stream pyramid for medical image segmentation, Biomed. Signal Process. Control 81 (2023) 104437.

[27] L. Zhang, K. Zhang, H. Pan, SUNet++: A deep network with channel attention for small-scale object segmentation on 3D medical images, Tsinghua Sci. Technol. 28 (4) (2023) 628–638.

[28] B. Zhan, E. Song, H. Liu, Z. Gong, G. Ma, C.-C. Hung, CFNet: A medical image segmentation method using the multi-view attention mechanism and adaptive fusion strategy, Biomed. Signal Process. Control 79 (2023) 104112.

[29] Y. Zhang, R. Jiao, Q. Liao, D. Li, J. Zhang, Uncertainty-guided mutual consistency learning for semi-supervised medical image segmentation, Artif. Intell. Med. 138 (2023) 102476.

[30] A. Deshpande, A novel approach to enhance effectiveness of image segmentation techniques on extremely noisy medical images BT - recent trends in image processing and pattern recognition, 2023, pp. 91–119.

[31] Q. He, Q. Yang, M. Xie, HCTNet: A hybrid CNN-transformer network for breast ultrasound image segmentation, Comput. Biol. Med. 155 (2023) 106629.

[32] F. Milletari, N. Navab, S.-A. Ahmadi, V-net: Fully convolutional neural networks for volumetric medical image segmentation, in: 2016 Fourth International Conference on 3D Vision (3DV), 2016, pp. 565–571.

[33] P. Tang, P. Yang, D. Nie, X. Wu, J. Zhou, Y. Wang, Unified medical image segmentation by learning from uncertainty in an end-to-end manner, Knowl.-Based Syst. 241 (2022) 108215.

[34] P. Ashtari, D.M. Sima, L. De Lathauwer, D. Sappey-Marinier, F. Maes, S. Van Huffel, Factorizer: A scalable interpretable approach to context modeling for medical image segmentation, Med. Image Anal. 84 (2023) 102706.

[35] Y. Zhang, X. Pan, C. Li, T. Wu, 3D liver and tumor segmentation with CNNs based on region and distance metrics, Appl. Sci. 10 (11) (2020) 3794.

[36] DREAM, The Digital Mammography DREAM Challenge, DREAM, 2016, [Online]. Available: https://bsmn.synapse.org/Explore/Data.

[37] CAMELYON16, 2021, [Online]. Available: https://camelyon16.grand-challenge.org/. [Accessed: 11-Dec-2021].

[38] D. Racoceanu, F. Capron, Semantic integrative digital pathology: Insights into microsemiological semantics and image analysis scalability, Pathobiology 83 (2–3) (2016) 148–155.

[39] iciar, 2018-Challenge.grand-challenge, 2021, [Online]. Available: https://iciar2018-challenge.grand-challenge.org/Dataset/. [Accessed: 11-Oct-2021].

[40] I.C. Moreira, I. Amaral, I. Domingues, A. Cardoso, M.J. Cardoso, J.S. Cardoso, INbreast: Toward a full-field digital mammographic database, Acad. Radiol. 19 (2) (2012) 236–248.

[41] CAMELYON17, 2021, [Online]. Available: https://camelyon17.grand-challenge.org/. [Accessed: 17-Dec-2021].

[42] J. Irvin, P. Rajpurkar, M. Ko, Y. Yu, S. Ciurea-Ilcus, C. Chute, H. Marklund, B. Haghgoo, R. Ball, K. Shpanskaya, J. Seekins, D.A. Mong, S.S. Halabi, J.K. Sandberg, R. Jones, D.B. Larson, C.P. Langlotz, B.N. Patel, M.P. Lungren, A.Y. Ng, CheXpert: A large chest radiograph dataset with uncertainty labels and expert comparison, 2019.

[43] A.E.W. Johnson, T.J. Pollard, N.R. Greenbaum, M.P. Lungren, C. Deng, Y. Peng, Z. Lu, R.G. Mark, S.J. Berkowitz, S. Horng, MIMIC-CXR-JPG, a large publicly available database of labeled chest radiographs, 14, (2019) 1–7.

[44] P.F. Raudaschl, P. Zaffino, G.C. Sharp, M.F. Spadea, A. Chen, B.M. Dawant, T. Albrecht, T. Gass, C. Langguth, M. Lüthi, et al., Evaluation of segmentation methods on head and neck CT: auto-segmentation challenge 2015, Med. Phys. 44 (5) (2017) 2020–2036.

[45] Pet-radiomics-challenges, 2021, [Online]. Available: https://www.kaggle.com/c/pet-radiomics-challenges/data. [Accessed: 28-Dec-2021].

[46] Data-science-bowl-2017, 2021, [Online]. Available: https://www.kaggle.com/c/data-science-bowl-2017. [Accessed: 14-Jul-2021].

[47] S.G. Armato III, G. McLennan, L. Bidaut, M.F. McNitt-Gray, C.R. Meyer, A.P. Reeves, B. Zhao, D.R. Aberle, C.I. Henschke, E.A. Hoffman, et al., The lung image database consortium (LIDC) and image database resource initiative (IDRI): a completed reference database of lung nodules on CT scans, Med. Phys. 38 (2) (2011) 915–931.

[48] Lung nodule analysis, 2020, [Online]. Available: https://lumic.grand-challenge.org/. [Accessed: 11-May-2020].

[49] Lung nodule analysis-2016, 2020, [Online]. Available: https://luna16.grand-challenge.org/. [Accessed: 11-May-2020].

[50] J. Borovec, A. Munoz-Barrutia, J. Kybic, Benchmarking of image registration methods for differently stained histological slides, in: 2018 25th IEEE International Conference on Image Processing, ICIP, 2018, pp. 3368–3372.

[51] Mild traumatic brain injury outcome prediction, 2021, [Online]. Available: https://tbichallenge.wordpress.com/data/. [Accessed: 11-Dec-2021].

[52] B.H. Menze, A. Jakab, S. Bauer, J. Kalpathy-Cramer, K. Farahani, J. Kirby, Y. Burren, N. Porz, J. Slotboom, R. Wiest, et al., The multimodal brain tumor image segmentation benchmark (BRATS), IEEE Trans. Med. Imaging 34 (10) (2014) 1993–2024.

[53] Grand challenge on MR brain segmentation at MICCAI 2018, 2021, [Online]. Available: https://mrbrains18.isi.uu.nl/data/. [Accessed: 13-Dec-2021].

[54] RIRE, 2020, [Online]. Available: http://insight-journal.org/rire/index.php. [Accessed: 14-May-2020].

[55] Multi-modality, lower spine 3D, 2020, [Online]. Available: https://projects.iq.harvard.edu/cdmri2018/data. [Accessed: 11-May-2020].

[56] Curious2018.grand-challenge, 2021, [Online]. Available: https://curious2018.grand-challenge.org/Data/. [Accessed: 11-Sep-2021].

[57] Tadpole.grand-challenge, 2021, [Online]. Available: https://tadpole.grandchallenge.org. [Accessed: 27-Sep-2021].

[58] idrid.grand-challenge.org. [Online]. Available: https://idrid.grand-challenge.org/Data.

[59] J. Staal, M.D. Abràmoff, M. Niemeijer, M.A. Viergever, B. Van Ginneken, Ridge-based vessel segmentation in color images of the retina, IEEE Trans. Med. Imaging 23 (4) (2004) 501–509.

[60] DRIVE, 2021, [Online]. Available: https://drive.grand-challenge.org/. [Accessed: 30-Sep-2021].

[61] Retouch.grand-challenge, 2021, [Online]. Available: https://retouch.grandchallenge.org. [Accessed: 11-May-2021].

[62] Automated cardiac diagnosis challenge -2017, 2021, [Online]. Available: https://www.creatis.insa-lyon.fr/Challenge/acdc/databases.html. [Accessed: 20-Sep-2021].

[63] ECG rhythm classification, 2021, [Online]. Available: https://irhythm.github.io/cardiol_test_set/. [Accessed: 23-May-2021].

[64] Computed tomography pulmonary angiograms CTPA, 2020, [Online]. Available: http://www.cad-pe.org/?page_id=12. [Accessed: 11-May-2020].

[65] Challenge on liver ultrasound tracking, 2021, [Online]. Available: https://clust.ethz.ch/. [Accessed: 15-Aug-2021].

[66] A.E. Kavur, N.S. Gezer, M. Barış, S. Aslan, P.-H. Conze, V. Groza, D.D. Pham, S. Chatterjee, P. Ernst, S. Özkan, et al., CHAOS challenge-combined (CT-MR) healthy abdominal organ segmentation, Med. Image Anal. 69 (2021) 101950.

[67] N. Heller, N. Sathianathen, A. Kalapara, E. Walczak, K. Moore, H. Kaluzniak, J. Rosenberg, P. Blake, Z. Rengel, M. Oestreich, J. Dean, M. Tradewell, A. Shah, R. Tejpaul, Z. Edgerton, M. Peterson, S. Raza, S. Regmi, N. Papanikolopoulos, C. Weight, The KiTS19 challenge data: 300 kidney tumor cases with clinical context, CT semantic segmentations, and surgical outcomes, 2019, pp. 1–13.

[68] Analysis of images to detect abnormalities in endoscopy accessed, 2021, [Online]. Available: https://isbi-aida.grand-challenge.org/. [Accessed: 20-Oct-2021].

[69] P. Rajpurkar, J. Irvin, A. Bagul, D. Ding, T. Duan, H. Mehta, B. Yang, K. Zhu, D. Laird, R.L. Ball, C. Langlotz, K. Shpanskaya, M.P. Lungren, A.Y. Ng, MURA: Large dataset for abnormality detection in musculoskeletal radiographs, 2017.

[70] Lower spine 3D multi-modality MRI data sets, 2021, [Online]. Available: https://ivdm3seg.weebly.com/data.html. [Accessed: 20-Oct-2021].

[71] S.S. Halabi, L.M. Prevedello, J. Kalpathy-Cramer, A.B. Mamonov, A. Bilbily, M. Cicero, I. Pan, L.A. Pereira, R.T. Sousa, N. Abdala, et al., The RSNA pediatric bone age machine learning challenge, Radiology 290 (2) (2019) 498–503.

[72] N. Bien, P. Rajpurkar, R.L. Ball, J. Irvin, A. Park, E. Jones, M. Bereket, B.N. Patel, K.W. Yeom, K. Shpanskaya, S. Halabi, E. Zucker, G. Fanton, D.F. Amanatullah, C.F. Beaulieu, G.M. Riley, R.J. Stewart, F.G. Blankenberg, D.B. Larson, R.H. Jones, C.P. Langlotz, A.Y. Ng, M.P. Lungren, Deep-learning-assisted diagnosis for knee magnetic resonance imaging: Development and retrospective validation of MRNet, PLoS Med. 15 (11) (2018) 1–19.

[73] L. Deleskog, N. Laursen, B.R. Nielsen, P. Schwarz, Vertebral fracture assessment by DXA is inferior to X-ray in clinical severe osteoporosis, Osteoporos. Int. 27 (7) (2016) 2317–2326.

[74] S. Rezaei, A. Emami, N. Karimi, S. Samavi, Gland segmentation in histopathological images by deep neural network, 1–5.

[75] N. Gessert, M. Nielsen, M. Shaikh, R. Werner, A. Schlaefer, Skin lesion classification using ensembles of multi-resolution EfficientNets with meta data, MethodsX 7 (2020) 100864.

[76] Skin cancer MNIST, 2021, [Online]. Available: https://www.kaggle.com/kmader/skin-cancer-mnist-ham10000. [Accessed: 04-Nov-2021].

[77] P. Bilic, P.F. Christ, E. Vorontsov, G. Chlebus, H. Chen, Q. Dou, C.-W. Fu, X. Han, P.-A. Heng, J. Hesser, et al., The liver tumor segmentation benchmark (lits), 2019, arXiv Prepr. arXiv:1901.04056.

[78] X. Liu, L. Yang, J. Chen, S. Yu, K. Li, Region-to-boundary deep learning model with multi-scale feature fusion for medical image segmentation, Biomed. Signal Process. Control 71 (2022) 103165.

[79] X. Yan, H. Tang, S. Sun, H. Ma, D. Kong, X. Xie, AFTer-UNet: Axial fusion transformer unet for medical image segmentation, in: Proceedings of the IEEE/CVF Winter Conference on Applications of Computer Vision, WACV, 2022, pp. 3971–3981.

[80] Z. Zhang, C. Wu, S. Coleman, D. Kerr, DENSE-inception U-net for medical image segmentation, Comput. Methods Programs Biomed. 192 (2020) 105395.

[81] Y. Al Khalil, S. Amirrajab, C. Lorenz, J. Weese, J. Pluim, M. Breeuwer, On the usability of synthetic data for improving the robustness of deep learning-based segmentation of cardiac magnetic resonance images, Med. Image Anal. 84 (2023) 102688.
[82] F. Yuan, Z. Zhang, Z. Fang, An effective CNN and transformer complementary network for medical image segmentation, Pattern Recognit. 136 (2023) 109228.
[83] Y. Wu, K. Liao, J. Chen, J. Wang, D.Z. Chen, H. Gao, J. Wu, D-former: a U-shaped dilated transformer for 3D medical image segmentation, Neural Comput. Appl. 35 (2) (2023) 1931–1944.
[84] L. Bonaldi, A. Pretto, C. Pirri, F. Uccheddu, C.G. Fontanella, C. Stecco, Deep learning-based medical images segmentation of musculoskeletal anatomical structures: A survey of bottlenecks and strategies, Bioengineering 10 (2) (2023).
[85] K. Chaitanya, E. Erdil, N. Karani, E. Konukoglu, Local contrastive loss with pseudo-label based self-training for semi-supervised medical image segmentation, Med. Image Anal. 87 (2023) 102792.
[86] C. Sridhar, P.K. Pareek, R. Kalidoss, S.S. Jamal, P.K. Shukla, S.J. Nuagah, Optimal medical image size reduction model creation using recurrent neural network and GenPSOWVQ, J. Healthc. Eng. 2022 (2022) 2354866.
[87] H. Wang, S. Xie, L. Lin, Y. Iwamoto, X.-H. Han, Y.-W. Chen, R. Tong, Mixed transformer U-net for medical image segmentation, in: ICASSP 2022-2022 IEEE International Conference on Acoustics, Speech and Signal Processing, ICASSP, 2022, pp. 2390–2394.
[88] S. Ren, K. He, R. Girshick, J. Sun, Faster r-cnn: Towards real-time object detection with region proposal networks, Adv. Neural Inf. Process. Syst. 28 (2015) 91–99.
[89] A. Ismail, T. Rahmat, S. Aliman, Chest X-ray image classification using faster R-CNN, Malays. J. Comput. 4 (1) (2019) 225–236.
[90] E.M.A. Anas, P. Mousavi, P. Abolmaesumi, A deep learning approach for real time prostate segmentation in freehand ultrasound guided biopsy, Med. Image Anal. 48 (2018) 107–116.
[91] V.D.P. Jasti, A.S. Zamani, K. Arumugam, M. Naved, H. Pallathadka, F. Sammy, A. Raghuvanshi, K. Kaliyaperumal, Computational technique based on machine learning and image processing for medical image analysis of breast cancer diagnosis, Secur. Commun. Netw. 2022 (2022) 1918379.
[92] P. Kora, C.P. Ooi, O. Faust, U. Raghavendra, A. Gudigar, W.Y. Chan, K. Meenakshi, K. Swaraja, P. Plawiak, U. Rajendra Acharya, Transfer learning techniques for medical image analysis: A review, Biocybern. Biomed. Eng. 42 (1) (2022) 79–107.
[93] B.D. de Vos, F.F. Berendsen, M.A. Viergever, H. Sokooti, M. Staring, I. Išgum, A deep learning framework for unsupervised affine and deformable image registration, Med. Image Anal. 52 (2019) 128–143.
[94] J. Chen, E.C. Frey, Y. He, W.P. Segars, Y. Li, Y. Du, TransMorph: Transformer for unsupervised medical image registration, Med. Image Anal. 82 (2022) 102615.
[95] B.A. Skourt, A. El Hassani, A. Majda, Lung CT image segmentation using deep neural networks, Procedia Comput. Sci. 127 (2018) 109–113.
[96] F.T. Ferreira, P. Sousa, A. Galdran, M.R. Sousa, A. Campilho, End-to-end supervised lung lobe segmentation, in: 2018 International Joint Conference on Neural Networks, IJCNN, 2018, pp. 1–8.
[97] Y. Oh, S. Park, J.C. Ye, Deep learning covid-19 features on cxr using limited training data sets, IEEE Trans. Med. Imaging 39 (8) (2020) 2688–2700.
[98] F. Ucar, D. Korkmaz, COVIDiagnosis-Net: Deep Bayes-SqueezeNet based diagnosis of the coronavirus disease 2019 (COVID-19) from X-ray images, Med. Hypotheses 140 (2020) 109761.
[99] X. Wu, H. Hui, M. Niu, L. Li, L. Wang, B. He, X. Yang, L. Li, H. Li, J. Tian, et al., Deep learning-based multi-view fusion model for screening 2019 novel coronavirus pneumonia: A multicentre study, Eur. J. Radiol. 128 (2020) 109041.
[100] H. Behzadi-Khormouji, H. Rostami, S. Salehi, T. Derakhshande-Rishehri, M. Masoumi, S. Salemi, A. Keshavarz, A. Gholamrezanezhad, M. Assadi, A. Batouli, Deep. learning, Reusable and problem-based architectures for detection of consolidation on chest X-ray images, Comput. Methods Programs Biomed. 185 (2020) 105162.
[101] A. Mittal, D. Kumar, M. Mittal, T. Saba, I. Abunadi, A. Rehman, S. Roy, Detecting pneumonia using convolutions and dynamic capsule routing for chest X-ray images, Sensors 20 (4) (2020) 1068.
[102] S. Sabour, N. Frosst, G.E. Hinton, Dynamic routing between capsules, 2017, arXiv Prepr. arXiv:1710.09829.
[103] R. Boddeda, S.V. Deepak, S.A. Patel, et al., A novel strategy for COVID-19 classification from chest X-ray images using deep stacked-ensembles, 2020, arXiv Prepr. arXiv:2010.05690.
[104] R. Wang, S. Chen, C. Ji, J. Fan, Y. Li, Boundary-aware context neural network for medical image segmentation, Med. Image Anal. 78 (2022) 102395.
[105] D. Nagasato, H. Tabuchi, H. Masumoto, H. Enno, N. Ishitobi, M. Kameoka, M. Niki, Y. Mitamura, Automated detection of a nonperfusion area caused by retinal vein occlusion in optical coherence tomography angiography images using deep learning, PLoS One 14 (11) (2019) e0223965.
[106] K. Simonyan, A. Zisserman, Very deep convolutional networks for large-scale image recognition, 2014, arXiv Prepr. arXiv:1409.1556.
[107] Y. Wu, Y. Xia, Y. Song, Y. Zhang, W. Cai, NFN+: A novel network followed network for retinal vessel segmentation, Neural Netw. 126 (2020) 153–162.
[108] H. Riaz, J. Park, H. Choi, H. Kim, J. Kim, Deep and densely connected networks for classification of diabetic retinopathy, Diagnostics 10 (1) (2020) 24.
[109] B.H.M. van der Velden, H.J. Kuijf, K.G.A. Gilhuijs, M.A. Viergever, Explainable artificial intelligence (XAI) in deep learning-based medical image analysis, 2021, arXiv Prepr. arXiv:2107.10912.
[110] Y.D. Kim, K.J. Noh, S.J. Byun, S. Lee, T. Kim, L. Sunwoo, K.J. Lee, S.-H. Kang, K.H. Park, S.J. Park, Effects of hypertension, diabetes, and smoking on age and sex prediction from retinal fundus images, Sci. Rep. 10 (1) (2020) 1–14.
[111] C. Spampinato, S. Palazzo, D. Giordano, M. Aldinucci, R. Leonardi, Deep learning for automated skeletal bone age assessment in X-ray images, Med. Image Anal. 36 (2017) 41–51.
[112] D.-H. Lee, et al., Pseudo-label: The simple and efficient semi-supervised learning method for deep neural networks, in: Workshop on Challenges in Representation Learning, ICML, Vol. 3, 2013, no. 2.
[113] D.B. Larson, M.C. Chen, M.P. Lungren, S.S. Halabi, N.V. Stence, C.P. Langlotz, Performance of a deep-learning neural network model in assessing skeletal maturity on pediatric hand radiographs, Radiology 287 (1) (2018) 313–322.
[114] S. Koitka, A. Demircioglu, M.S. Kim, C.M. Friedrich, F. Nensa, Ossification area localization in pediatric hand radiographs using deep neural networks for object detection, PLoS One 13 (11) (2018) e0207496.
[115] S.H. Tajmir, H. Lee, R. Shailam, H.I. Gale, J.C. Nguyen, S.J. Westra, R. Lim, S. Yune, M.S. Gee, S. Do, Artificial intelligence-assisted interpretation of bone age radiographs improves accuracy and decreases variability, Skeletal Radiol. 48 (2) (2019) 275–283.
[116] Y. LeCun, et al., Generalization and network design strategies, Connect. Perspect. 19 (1989) 143–155.
[117] V.I. Iglovikov, A. Rakhlin, A.A. Kalinin, A.A. Shvets, Paediatric bone age assessment using deep convolutional neural networks, in: Lect. Notes Comput. Sci. (Including Subser. Lect. Notes Artif. Intell. Lect. Notes Bioinformatics), in: LNCS, vol. 11045, 2018, pp. 300–308.
[118] J.C. Castillo, Y. Tong, J. Zhao, F. Zhu, RSNA bone-age detection using transfer learning and attention mapping, 2018.
[119] P. Van Molle, M. De Strooper, T. Verbelen, B. Vankeirsbilck, P. Simoens, B. Dhoedt, Visualizing convolutional neural networks to improve decision support for skin lesion classification, in: Understanding and Interpreting Machine Learning in Medical Image Computing Applications, Springer, 2018, pp. 115–123.
[120] I. Kandel, M. Castelli, A. Popovič, Musculoskeletal images classification for detection of fractures using transfer learning, J. Imaging 6 (11) (2020) 127.
[121] H. Lee, S. Tajmir, J. Lee, M. Zissen, B.A. Yeshiwas, T.K. Alkasab, G. Choy, S. Do, Fully automated deep learning system for bone age assessment, J. Digit. Imaging 30 (4) (2017) 427–441.
[122] T. Van Steenkiste, J. Ruyssinck, O. Janssens, B. Vandersmissen, F. Vandecasteele, P. Devolder, E. Achten, S. Van Hoecke, D. Deschrijver, T. Dhaene, Automated assessment of bone age using deep learning and Gaussian process regression, in: Proc. Annu. Int. Conf. IEEE Eng. Med. Biol. Soc. EMBS, Vol. 2018-July, 2018, pp. 674–677.
[123] R. Mishra, O. Daescu, P. Leavey, D. Rakheja, A. Sengupta, Histopathological diagnosis for viable and non-viable tumor prediction for osteosarcoma using convolutional neural network, in: International Symposium on Bioinformatics Research and Applications, 2017, pp. 12–23.
[124] S. Mahore, K. Bhole, S. Rathod, Machine learning approach to classify and predict different osteosarcoma types, in: 2021 8th International Conference on Signal Processing and Integrated Networks, SPIN, 2021, pp. 641–645.
[125] B.H.M. van der Velden, H.J. Kuijf, K.G.A. Gilhuijs, M.A. Viergever, Explainable artificial intelligence (XAI) in deep learning-based medical image analysis, Med. Image Anal. 79 (2022) 102470.
[126] B. Davazdahemami, H.M. Zolbanin, D. Delen, An explanatory analytics framework for early detection of chronic risk factors in pandemics, Healthc. Anal. 2 (2022) 100020.
[127] H.B. Arunachalam, R. Mishra, O. Daescu, K. Cederberg, D. Rakheja, A. Sengupta, D. Leonard, R. Hallac, P. Leavey, Viable and necrotic tumor assessment from whole slide images of osteosarcoma using machine-learning and deep-learning models, PLoS One 14 (4) (2019) 1–19.
[128] M. D'Acunto, M. Martinelli, D. Moroni, Deep learning approach to human osteosarcoma cell detection and classification, in: International Conference on Multimedia and Network Information System, 2018, pp. 353–361.
[129] R. Sayres, A. Taly, E. Rahimy, K. Blumer, D. Coz, N. Hammel, J. Krause, A. Narayanaswamy, Z. Rastegar, D. Wu, et al., Using a deep learning algorithm and integrated gradients explanation to assist grading for diabetic retinopathy, Ophthalmology 126 (4) (2019) 552–564.